

Duobinary modulation/predistortion techniques effects on high bit rate radio over fiber systems

Mahmoud M. A. Eid¹, Ashraf S. Selim², Ahmed Nabih Zaki Rashed³, Abd El-Naser A. Mohammed⁴, Mohamed Yassin Ali⁵, Shaimaa S. Abaza⁶

¹Department of Electrical Engineering, College of Engineering, Taif University, Kingdom of Saudi Arabia

^{3,4}Electronics and Electrical Communications Engineering Department, Faculty of Electronic Engineering, Menoufia University, Menouf, Egypt

^{2,5,6}Benha Faculty of Engineering, Benha University, Benha, Egypt

Article Info

Article history:

Received Jun 29, 2020

Revised Sep 3, 2020

Accepted Sep 18, 2020

Keywords:

Duo-Binary modulation

Local area network

Predistortion technique

RoF

ABSTRACT

The work has presented duobinary modulation and predistortion techniques for the radio over fiber system enhancement for achieving security level. Duobinary modulation technique has more compact modulated spectral linewidth with standard non return to zero modulation code. Different NRZ/RZ rectangle shape employed that are namely exponential rectangle shape (ERS), and Gaussian rectangle shape (GRS) for different transmission bit rates. Switching bias voltage, and switching RF voltage based LiNbO3 modulator are changed to measure the performance parameters of the radio over fiber (RoF) system. Predistortion technique improves the linearity of transmitter amplifiers and it is considered as a power efficiency technique. The optimum values of the Q-factor, data error rate (BER), electrical power, signal gain, noise figure, and light signal/noise ratio are achieved with 8 Volt for both switching biases/switching RF signal at 100 GHz. Signal quality/BER and electrical power after the receiver enhancement ratio by using this technique at different RF signal frequencies.

This is an open access article under the [CC BY-SA](https://creativecommons.org/licenses/by-sa/4.0/) license.



Corresponding Author:

Ahmed Nabih Zaki Rashed

Faculty of Electronic Engineering, Menoufia University

Menouf 32951, Egypt

E-mail: ahmed_733@yahoo.com

1. INTRODUCTION

They presented the RoF network model with the investigation of Q-factor, BER and eye-opening with optic fiber length, operating signal wavelength, and bit rate. The radio frequency signal is 10 GHz with a data rate of up to 3 Gb/s and is used in this model through fiber length up to 50 km. This study shows that the RZ modulation code is better than the NRZ modulation code in the high power regime [1, 2, 3-9]. They clarified the simulation modeling of RoF for home network applications using different line coding. Performance parameters evaluation is summarized such as Q-factor, BER, eye height, and threshold value with respect to transmission bit rate and fiber cable length under different line coding schemes [3, 10-15].

Different electrical encoding methods and different optical modulation schemes are analyzed. Different wavelength division multiplexing, optical add/drop multiplexers are performed with the optimization of fiber cable length. The signal spectrum for both base stations is measured with the testing of the Q-factor and BER analyzer. As well as 8 channels are multiplexed and routed using wavelength selective optical add/drop multiplexer which is used as fiber Bragg grating filter [4, 5, 16-20]. Refs. [5, 6, 21-24] presented the filtration techniques that are employed for amplitude noise reduction based millimeter RoF

communication [7, 8, 25-28]. The max quality factor and min data error rate are tested for different optical receivers (PIN, and APD photodetectors) with different types of noise (shot noise, and thermal noise). RoF systems is stimulated based on NRZ coding for a bit rate of 2.5 Gb/s [29-37].

2. MODEL DESCRIPTION AND RESEARCH METHOD

We have developed the previous work in Ref. [6] to enhance radio over fiber-based local area communication network. By creating non return to zero duobinary signal using a precoder and a duobinary pulse generator, so the duobinary signal can be generated. Pseudo random bit sequence generator to generate a random stream of bits. This stream is encoded in the configuration of return to zero code. The encoded signal can be directed to distortion generator which treats the signal nonlinearity. The generator derived the first LiNbO₃ Mach Zehnder modulator and then concatenates this modulator with the second modulator driven by an electrical sinusoidal signal that has a clock frequency equal to the transmission data rate of 100 GHz. For the high-speed data transmission system, the clock frequency defines the transmission limit within the range of 10 GHz to 250 GHz. The duobinary used a dedicated precoder at the transmitter that makes the receiver can use direct detection mechanism. The signal is directed from modulator to EDFA amplifier for amplification then into the single-mode fiber which its length of 20 km. The routed signal from single-mode fiber cable is traveled to APD photodetector to convert the light signal to an electrical signal. The converted signal is treated from ripples through low pass Bessel filter and the Q factor and min BER are tested by bit error rate analyzer.

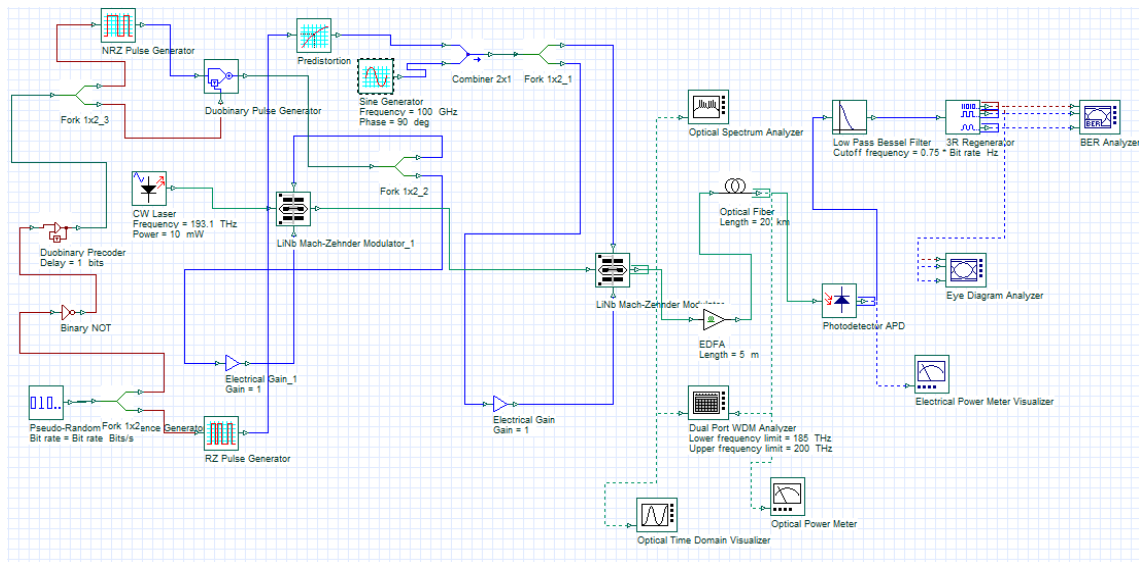


Figure 1. Schematic view of duobinary radio over fiber simulation modeling

There are many measurements after modulator and single-mode fiber cable to measure the RoF system operation performance. Dual-port WDM analyzer is used to measure the signal gain, noise figure, and optical signal to noise ratio. The optical power meter measures optical power into the fiber cable. The optical spectrum analyzer measures the modulated power on the vertical scale and the operating signal wavelength on the horizontal scale. As well as optical time-domain visualizer measures the modulated power with a bit time. Both BER analyzer and eye diagram analyzer to test the maxi. Q-factor and min. bit error rate at the receiver side.

3. PERFORMANCE ANALYSIS WITH DISCUSSIONS

Stimulated the duo-binary modulation and predistortion techniques are analyzed for the enhancement of radio over fiber communication systems for local area network applications with different transmission bit rates. Switching bias voltage and switching RF voltage are changed to reach the optimum value in order to achieve maximum quality factor enhancement and BER reduction in addition to the enhancement of electrical received power. The deduced figures are assured the obtained results:

Figures 2 and 3 show the relation between max Q-factor and min bit error rate in relation to different NRZ/RZ rectangle shape. It is observed that the NRZ/RZ (ERS) configuration has presented maxi. Q-factor and min. BER that NRZ/RZ (GRS) configuration at 10 Gb/s, while NRZ/RZ (GRS) configuration has presented max. Q-factor and min. BER than NRZ/RZ (ERS) configuration at 40 Gb/s. The max. Q factor is 5.8 for the NRZ/RZ (ERS) configuration with 40 Gb/s, 6.5 for the NRZ/RZ (GRS) configuration with the same bit rate. The max. Q factor is 8.654 for the NRZ/RZ (ERS) configuration with 10 Gb/s, 8.2435 for the NRZ/RZ (GRS) configuration with the same bit rate. The min. BER is 1.5×10^{-10} for NRZ/RZ (ERS) configuration with 40 Gb/s, 0.9×10^{-10} for the NRZ/RZ (GRS) configuration with the same bit rate. The min. BER is 13.5×10^{-12} for the NRZ/RZ (ERS) configuration with 10 Gb/s, 6.5×10^{-12} for the NRZ/RZ (GRS) configuration with the same data rate.

Figure 4 indicates that the variations of electrical power after APD with different NRZ/RZ rectangle shape at various bit rates. The NRZ/RZ (GRS) configuration has presented larger electrical power at the receiver in compared with NRZ/RZ (ERS) configuration. The received power is 5.5 mW for the NRZ/RZ (ERS) configuration with 40 Gb/s, 6.3 mW for the NRZ/RZ (GRS) configuration with the same bit rate. The received power is 18.654 mW for the NRZ/RZ (ERS) configuration with 10 Gb/s, 19.2 mW for the NRZ/RZ (GRS) configuration with the same bit rate. Figure 5 demonstrates that the maximum Q-factor in relation to RF signal frequency with/without predistortion technique. It is inferred that the important role of predistortion technique in upgrading signal quality factor. The max. Q Factor is 8 with predistortion, 2.2 without predistortion at 10 Gb/s. The max. Q Factor is 5.5 with predistortion, 2.8 without predistortion at 40 Gb/s. The max. Q Factor is 7.8 with predistortion, 2.1 without predistortion at 100 Gb/s. The max. Q Factor is 8.354 with predistortion, 2.02 without predistortion at 160 Gb/s. The max. Q Factor is 7.354 with predistortion, 2.01 without predistortion at 250 Gb/s. Figures 6 and 7 show max. Q-factor variations with switching bias voltage and switching RF voltage. It is indicated that the optimum value of the maximum Q-factor is achieved at 8 Volt for both switching cases of the modulator. As shown in Figure 6, the max. Q factor is 2.1 at 4 V switching bias voltage. The max. Q factor is 14.8 at 8 V switching bias voltage. The max. Q factor is 5 at 12 V switching bias voltage. The max. Q factor is 4 at 16 V switching bias voltage. the max. Q factor is 3 at 20 V switching bias voltage. As shown in Figure 7, the max. Q factor is 2.225 at 4 V switching RF voltage. The max. Q factor is 2.775 at 8 V switching RF voltage. The max. Q factor is 2.7 at 12 V switching RF voltage. The max. Q factor is 2.654 at 16 V switching RF voltage. the max. Q factor is 2.554 at 20 V switching RF voltage.

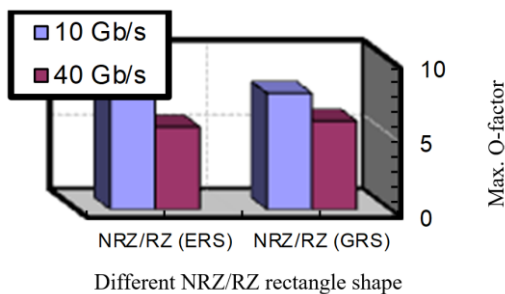


Figure 2. Variations of max Q-factor with overall system bit-rate based on different NRZ/RZ rectangle shape

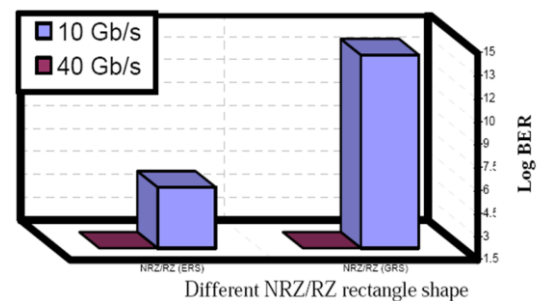


Figure 3. Min. data error rate variations versus overall system bit-rate based on different NRZ/RZ rectangle shape

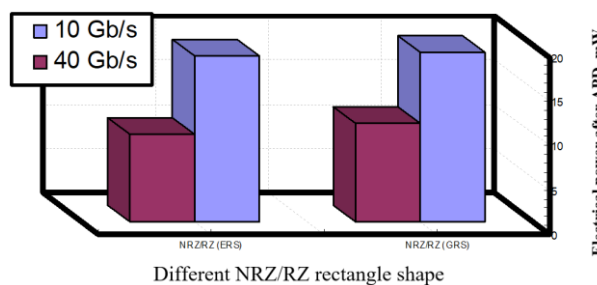


Figure 4. Electrical power after APD with overall system bit-rate based on different NRZ/RZ rectangle shape

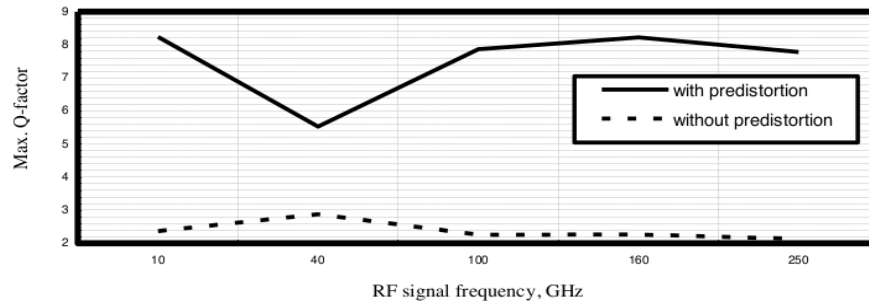


Figure 5. Max. Q-factor versus RF signal frequency in the presence and absence of the predistortion technique

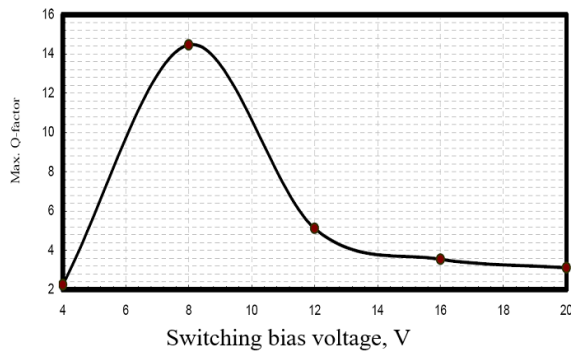


Figure 6. Variations of max. Q-factor against variations of switching bias voltage based LiNbO₃ Mach Zehnder Modulator at RF signal frequency of 100 GHz

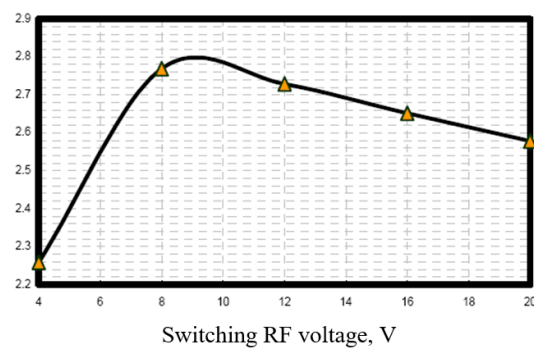


Figure 7. Max. Q-factor with switching voltage based LiNbO₃ Mach Zehnder Modulator at RF frequency of 100 GHz

Figures 8-11 indicate that the gain, noise figure, electrical power, and light signal/noise ratio with the switching bias voltage and switching RF voltage. The oscillation values between increasing and decreasing performance parameters under study. As shown in Figure 8, gain and noise figure are slightly decrease with the increase of the switching bias voltage. Also in the same way as clarified in Figure 9, gain and noise figure are slightly decrease with the increase of the switching RF voltage. As shown in Figure 10, electrical power and light signal to noise ratio are slightly decrease with the increase of the switching bias voltage. Also in the same way as clarified in Figure. 11, electrical power and light signal to noise ratio are slightly decrease with the increase of the switching RF voltage.

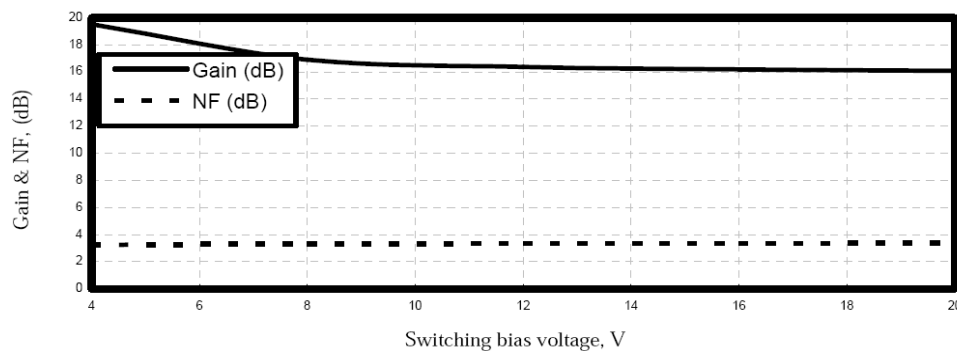


Figure 8. Gain, noise figure with switching bias voltage based LiNbO₃ Mach Zehnder Modulator at frequency of 100 GHz

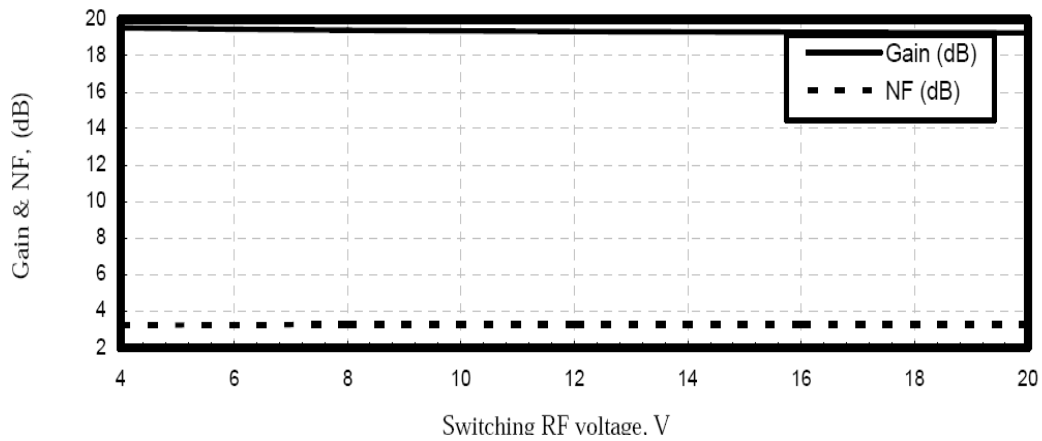


Figure 9. Gain, noise figure with switching RF voltage based LiNbO₃ Mach Zehnder Modulator at frequency of 100 GHz

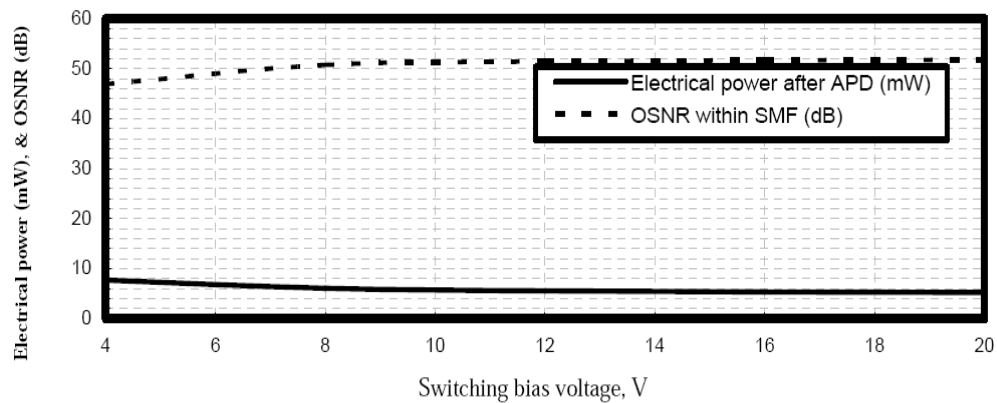


Figure 10. Variations of electrical power and light signal/noise ratio against variations of switching bias voltage based LiNbO₃ Mach Zehnder Modulator at RF signal frequency of 100 GHz

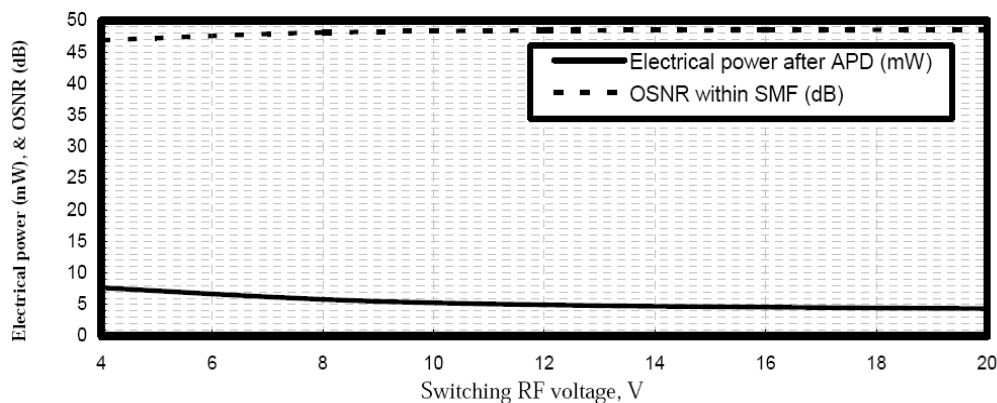


Figure 11. Electrical power and light signal/noise ratio versus switching RF voltage based LiNbO₃ Mach Zehnder Modulator at RF signal frequency of 100 GHz

Figures 12-15 show that eye diagram analyzer and BER analyzer for both NRZ/RZ (GRS) configuration, NRZ/RZ (ERS) configuration at different transmission bit rates. These graphs show the max Q-factor and min BER values exactly. The max. Q factor is 8.12, min. BER is 2.2×10^{-16} for NRZ/RZ (exponential rectangle shape) at 10 Gb/s as clarified in Figure 12. The max. Q factor is 5.53, min. BER is

1.504×10^{-8} for NRZ/RZ (exponential rectangle shape) at 40 Gb/s as clarified in Figure 13. The max. Q factor is 7.97, min. BER is 7.64×10^{-16} for NRZ/RZ (Gaussian rectangle shape) at 10 Gb/s as clarified in Figure 14. The max. Q factor is 5.92, min. BER is 1.445×10^{-9} for NRZ/RZ (Gaussian rectangle shape) at 40 Gb/s as clarified in Figure 15. Figures 16, and 17 demonstrate that the variations of maximum modulated power after LiNbO₃ Mach Zehnder modulator without/with predistortion technique at 40 Gb/s. The enhancement of modulated signal peak power after predistortion technique. The max. signal power is 1.312 dBm, noise power is -104.824 dBm without predistortion technique at 40 Gb/s as clarified in Figure 16. The max. signal power is 1.15548 dBm, noise power is -104.824 dBm with predistortion technique at 40 Gb/s as clarified in Figure 17.

Figure 18 shows that Q-factor enhancement ratio, electrical power enhancement ratio and BER reduction ratio in relation to RF signal frequency. The Q-factor enhancement ratio, BER reduction ratio is achieved at 250 GHz, while the electrical power enhancement ratio is achieved at 160 GHz. The Q-factor enhancement ratio is 71.26% at 10 GHz, 47.90% at 40 GHz, 71.28% at 100 GHz, 72.43% at 160 GHz, 72.69% at 250 GHz. Besides, the BER reduction ratio is 28.74% at 10 GHz, 52.10% at 40 GHz, 28.72% at 100 GHz, 27.57% at 160 GHz, 27.31% at 250 GHz. Moreover, the electrical power enhancement ratio is 2.2% at 10 GHz, 8.10% at 40 GHz, 58.41% at 100 GHz, 65.60% at 160 GHz, and 60.88% at 250 GHz.

The complete comparison between maximum Q-factor, minimum BER, and electrical power after APD photodiode in the presence and absence of predistortion technique is summarized in Table 1 at different RF signal frequencies. As well as the performance parameters enhancement ratio are summarized in Table 2 at different RF signal frequencies.

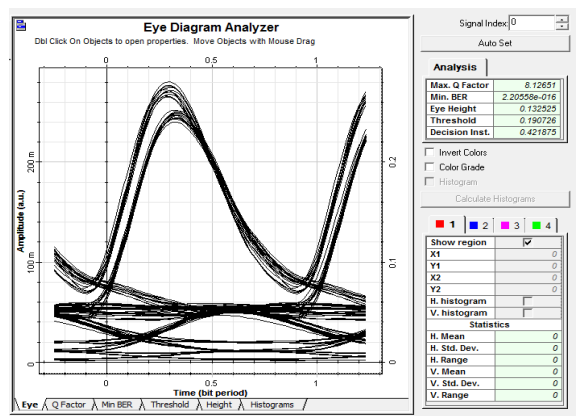


Figure 12. Eye diagram analyzer for NRZ/RZ (exponential rectangle shape) at 10 Gb/s

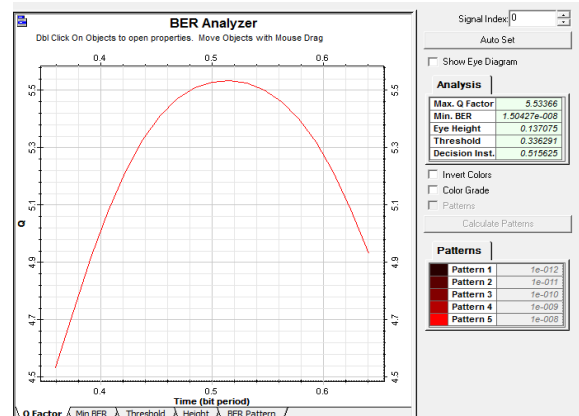


Figure 13. Bit error rate analyzer for NRZ/RZ (exponential rectangle shape) at 40 Gb/s

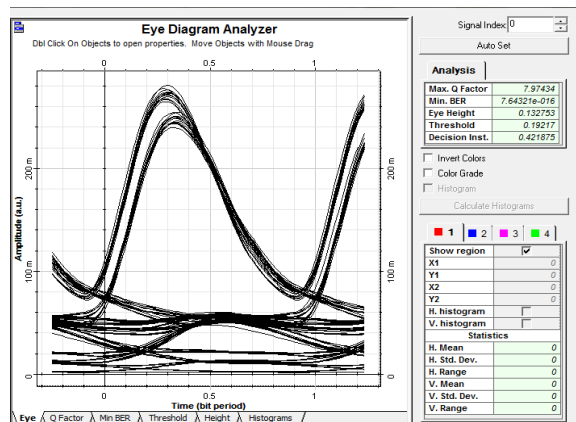


Figure 14. Eye diagram analyzer for NRZ/RZ (Gaussian rectangle shape) at 10 Gb/s

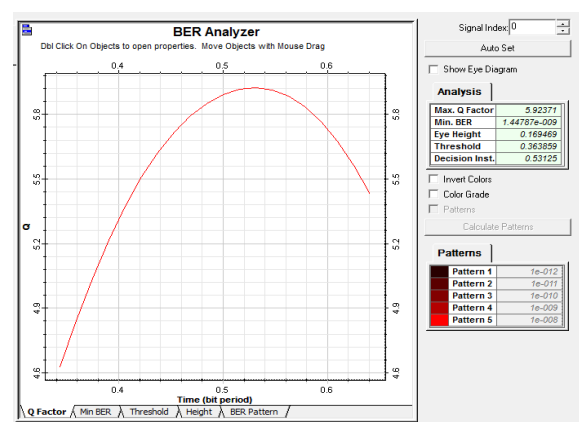


Figure 15. Eye diagram analyzer for NRZ/RZ (Gaussian rectangle shape) at 40 Gb/s

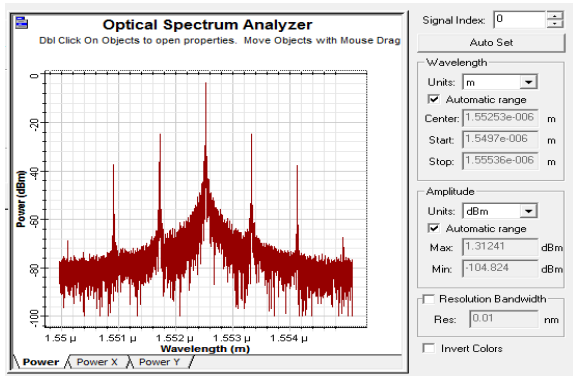


Figure 16. Max modulated power after LiNbO₃ MZM without predistortion technique at 40 Gb/s

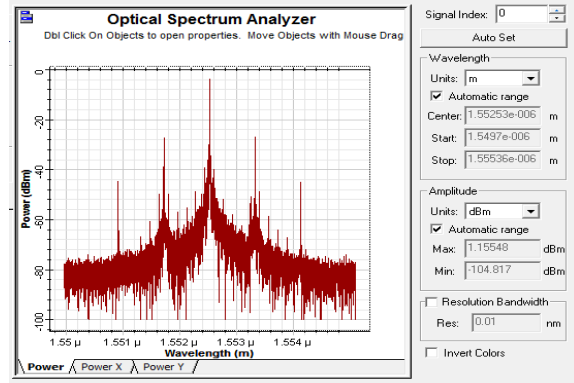


Figure 17. Maximum modulated power after LiNbO₃ Mach Zehender modulator in the presence of predistortion technique at 40 Gb/s

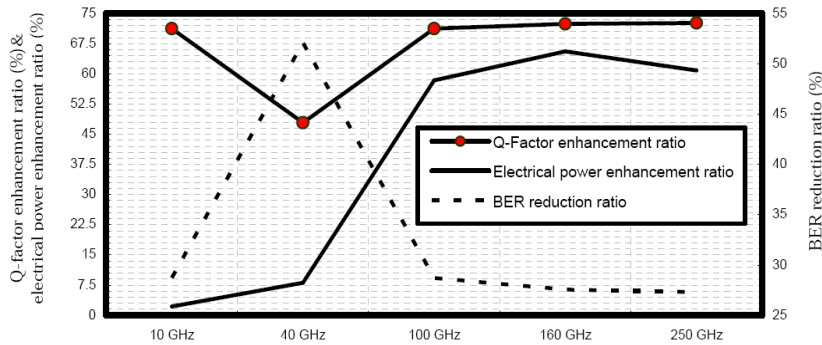


Figure 18. Q-factor enhancement ratio, electrical power enhancement ratio and BER reduction ratio in relation to RF signal frequency

Table 1. System performance parameters with/without predistortion technique

RF signal frequency	Without Predistortion technique			With Predistortion technique		
	Max. Q-factor	Min. BER	Electrical power after receiver (mW)	Max. Q-factor	Min. BER	Electrical power after receiver (mW)
10 GHz	2.367	0.00889	13.016	8.238	8.71×10^{-17}	13.31
40 GHz	2.881	0.0018844	9.098	5.53	1.5×10^{-8}	9.9
100 GHz	2.258	0.0118947	7.682	7.864	1.673×10^{-15}	18.472
160 GHz	2.267	0.011156	6.34	8.223	9.07×10^{-17}	18.432
250 GHz	2.128	0.0164218	7.324	7.794	2.9×10^{-15}	18.725

Table 2. System performance parameters enhancement ratio with predistortion technique

RF signal frequency	Q-factor enhancement ratio (%)	BER reduction ratio (%)	Electrical power enhancement ratio (%)
10 GHz	71.26	28.74	2.20
40 GHz	47.90	52.10	8.10
100 GHz	71.28	28.72	58.41
160 GHz	72.43	27.57	65.60
250 GHz	72.69	27.31	60.88

4. CONCLUSION

In summary, we have simulated the radio over fiber communication based local area optical networks using duo-binary modulation and predistortion techniques. It is denied inferred that the enhancement of both signal quality and its power, in addition to the reduction in bit error rate in the presence of predistortion technique. It is observed that the NRZ/RZ in GRS configuration has presented max. Q-factor

and min. BER at high data rates. It is efficient for electrical power saving. The optimum Q-factor is achieved at a value of 8 Volt for both switching bias voltage and switching RF voltage based Mach Zehnder modulator. In addition to the optical signal to noise ratio is slightly changed with the variations of both switching RF, switching bias voltages which belong to the modulator. It is indicated that the enhancement of modulated signal peak power to 1.15548 dBm with predistortion technique, while its value is degraded to 1.31241 dBm without predistortion technique. Finally, it is inferred that the maximum Q-factor enhancement ratio is reached to 72.69 %, the minimum BER reduction ratio is reached to 27.31 at 250 GHz, while maximum electrical power enhancement ratio is reached to 65.60 % at 160 GHz.

REFERENCES

- [1] Y. Okamura, and S. Yamamoto, "Ultra-Low Loss Single Mode Fiber Design for 2.5-6 μ m Band Absorption," *Applied Optics*, vol. 22, no. 19, pp. 3098-3101, 1983S.
- [2] S. S. Kumar, P. Keerthana, "Simulation of RoF using wavelength selective OADM," *International Journal of Research Studies in Science, Engineering and Technology*, vol. 2, no. 9, pp. 16-22, 2015.
- [3] N. Singh, H. Kaur, "Amplitude noise reduction in millimeter wave radio-over-fiber systems by using filtration techniques," *International Journal of Advanced Research in Computer and Communication Engineering*, vol. 5, no. 7, pp. 302-306, 2016.
- [4] K. Shrimali, A. Patel, "Performance analysis of ROF system using NRZ coding," *International Research Journal of Engineering and Technology (IRJET)*, vol. 4, no. 1, pp. 1568-1570, 2017.
- [5] A. A. Khadir, et al., "Achieving optical fiber communication experiments by optisystem," *International Journal of Computer Science and Mobile Computing*, vol. 3, no. 6, pp. 42-53, 2014.
- [6] H. Tokiwa, and Y. Mimura, "Ultra-low Loss Fluoride Glass Single Mode Fiber Design", *J. Lightwave Technol.*, vol. LT-4, pp. 1260-1266, 1986.
- [7] A. Gupta, "Comparative analysis of various wavelength division multiplexed PON standards," *Journal of Optical Communications*, vol. 40, no. 1, pp. 51-54, 2019.
- [8] A. Sheetal, H. Singh, "Cost Efficient 4 \times 2.5 Gb/s Transparent WDM Ring network using DML and metro core fiber for long reach applications," *Journal of Optical Communications*, vol. 40, no. 1, pp. 67-74, 2019.
- [9] S. Iyer, S. P. Singh, "Effect of channel spacing on the design of mixed line rate optical wavelength division multiplexed networks," *Journal of Optical Communications*, vol. 40, no. 1, pp. 75-82, 2019.
- [10] S. Driz, A. Djebbari, "Performance evaluation of sub-carrier multiplexed SAC-OCDMA system using optimal modulation index," *Journal of Optical Communications*, vol. 40, no. 1, pp. 83-92, 2019.
- [11] F. M. Ghannouchi, O. Hammi, "Behavioral modeling and predistortion," *IEEE Microwave Magazine*, vol. 10, no. 7, pp. 52-64, 2010.
- [12] F. Vendittia et al., "Fluorides decontamination by means of Aluminum polychloride based commercial coagulant", *J. of Water Process Engineering*, Vol. 26, pp. 182-186, 2018. D. Gustafsson, et al., "A wideband and compact GaN MMIC doherty amplifier for microwave link applications," *IEEE Transactions on Microwave Theory and Techniques*, vol. 61, no. 2, pp. 922-930, 2013.
- [13] W. J. Tomlinson and R. H. Stolen, "Nonlinear Phenomena in Optical Fibers", *IEEE Comm. Magazine*, Vol. 26, No. 4, pp. 36-44, 1988.
- [14] S. Mitachi and T. Miyashita, "Refractive Index Dispersion for BaF₂-GdF₃-ZrF₄-AlF₃ Glasses", *Applied Optics*, vol. 22, no. 16, pp. 2419-2425, 1983.
- [15] S. M. Nagia et al., "Fluoride release and recharge of enhanced resin modified glass monomer at different time intervals," *Future Dental Journal*, vol. 4, no. 2, pp. 221-222, 2018.
- [16] A. Zhu, et al., "Digital predistortion for envelope-tracking power amplifiers using decomposed piecewise Volterra series," *IEEE Trans. Microw. Theory Tech.*, vol. 56, no. 10, pp. 2237-2247, 2008.
- [17] S. S. Walker, "Rapid Modelling and Estimation of Total Spectral Loss in Optical Fibers," *J. Lightwave Technol.*, vol. LT-4, no. 8, pp. 1125-1137, 1986.
- [18] H. E. H. Ahmed et al., "On the Propagation Characteristics of Fluoride and Germania Doped Optical Fibers", *Ain Shams Univ. Eng. Bulletin*, vol. 27, no. 4, pp. 241-255 1992.
- [19] K. Kitayama et al., "Design Considerations for the Structural Optimization of a Single Mode Fiber", *J. Lightwave Technol.*, vol. LT-1, no. 2, pp. 363-369, 1983.
- [20] D. Wood, "Constraints on the Bit Rates in Direct Detection Optical Communication Systems Using Linear or Soliton Pulses," *J. Lightwave Technol.*, vol. 8, no. 7, pp. 1097-1106, 1990.
- [21] R. Sanjari and M. Pourmahyabadi, "Design of Single Mode Photonic Crystal Fiber with Outstanding Characteristics of Confinement Loss and Chromatic Dispersion over S and L Communication Band", *Iranian Journal of Electrical & Electronic Engineering*, vol. 12, no. 1, pp. 29-34, 2016.
- [22] F. Öhman, et al., "Noise and regeneration in semiconductor waveguides with saturable gain and absorption," *IEEE J. Quantum Electron.*, vol. 40, no. 3, pp. 245-255, 2004.
- [23] S. Iyer, S. P. Singh, "Effect of Channel Spacing on the Design of Mixed Line Rate Optical Wavelength Division Multiplexed Networks," *Journal of Optical Communications*, vol. 40, no. 1, pp. 75-82, 2019.
- [24] V. R. Miriamally, T. Hailu, "2D Single Mode Optical Fiber Wave Guide Design for Multi Haul Applications," *International Journal of Innovative Research in Electronics and Communications (IJIREC)*, vol. 3, no. 5, pp. 24-35, 2016, DOI: <http://dx.doi.org/10.20431/2349-4050.0305004>, www.arcjournals.org.

- [25] F. E. Seraji, R. Kiaee, "A Revisit of Refractive Index Profiles Design for Reduction of Positive Dispersion, Splice Loss, and Enhancement of Negative Dispersion in Optical Transmission Lines," *International Journal of Optics and Applications*, vol. 4, no. 2, pp. 62-67, 2014, DOI: 10.5923/j.optics.20140402.06.
- [26] S. A. Bhuiyan, "Design, Simulation, Performance Analysis and Optimization Process of MMGRIN Fiber with RI Distribution," *1st International conference on Electrical & Communication Engineering and Renewable Energy*, pp. 1-6, 2014.
- [27] M. Artiglia, "Mode field Diameter Measurements in Single Mode Optical Fibers," *Journal of Lightwave Tech.*, vol. 7, no. 8, pp. 1139-1152, 1989.
- [28] V. Palodiya, S. K. Raghuvanshi, "Dispersion Characteristics of Novel Class Multi Clad Dispersion Shifted Hollow Core Fibers for WDM Optical Systems," *Indian Journal of Pure & Applied Physics*, vol. 56, pp. 76-79, 2018.
- [29] Hazem M. El-Hageen, et al., "RZ line coding scheme with direct laser modulation for upgrading optical transmission systems," *Open Eng. Journal*, vol. 10, no. 1, pp. 546-551, 2020. <https://doi.org/10.1515/eng-2020-0066>.
- [30] Ahmed Nabih Zaki Rashed, et al., "High-speed signal processing and wide band optical semiconductor amplifier in the optical communication systems," *Journal of Optical Communications*, Published Online: 25 July 2020. <https://doi.org/10.1515/joc-2020-0070>.
- [31] C. Kromer et al., "A Low-Power 20-GHz 52-dB Transimpedance Amplifier in 80-nm CMOS," *IEEE Journal of Solid State Circuits*, vol. 39, no. 6, pp. 885-894, 2004.
- [32] D. Praveen, et al., "A Comparative Analysis of Transimpedance Amplifier in Giga-bit Optical Communication," *Research Journal of Engineering Sciences*, vol. 3, no. 3, pp. 6-9, 2014.
- [33] Lucas M. Riob, et al., "Wideband Transimpedance Amplifiers for Optoelectronics: Applications to Dynamic Interferometry," *Revista elektron*, vol. 1, no. 1, pp. 16-22, 2017.
- [34] L. Safar, M. S. Zaki, "Design and Simulation of Differential Transimpedance Amplifier (TIA) Based on 0.18 μm CMOS Technology," *Al-Rafidain Engineering*, vol. 21, no. 4, pp. 121-130, 2013.
- [35] X. Hui, et al., "A 3.125-Gb/s Inductor Less Transimpedance Amplifier for Optical Communication in 0.35 μm CMOS," *Journal of Semiconductors*, vol. 32, no. 10, pp. 105003 (1-6), 2011.
- [36] S. Subi, and G. b. Lakshmi, "Optical Solitons Simulation Using DSF and Optical Pulse Generator in Single Mode Optical Fiber," *International Journal of Science and Research (IJSR)*, ISSN (Online): 2319-7064, vol. 4, no. 2, pp. 254-258, 2015.
- [37] M. Arora and G. Pandove, "Simulated Circuit for Generation of 40 GHz Soliton Train," *International Journal of Emerging Trends in Electrical and Electronics (IJETEE – ISSN: 2320-9569)*, vol. 5, no. 2, pp. 73-76, 2013.